New Ordered Morphologies in ABC Triblock Copolymers

Clemens Auschra[†] and Reimund Stadler[*]

Institut für Organische Chemie, J. J. Becherweg 18-20, D-6500 Mainz, Germany

Received November 12, 1992

ABSTRACT: The morphology of well-defined poly(styrene-*b*-ethylene-*co*-1-butene-*b*-methyl methacrylate) (P(S-*b*-EB-*b*-MMA)) triblock copolymers of molecular weights of approximately 2×10^5 has been investigated by transmission electron microscopy. The fraction of the midblock varies, while the ratio of the outer blocks is kept approximately constant. A block copolymer with 38 wt % EB shows a lamellar morphology. Hitherto unknown morphologies were observed in the triblock copolymers with lower EB content. Regular EB cylinders located at the interface of PS and PMMA lamellae are formed at a level of 17 wt % EB. The triblock copolymer with 6 wt % EB shows PS cylinders dispersed in a PMMA matrix. The cylinders are covered with small isolated EB rings. These unexpected highly ordered structures result from the strong incompatibility between the EB midblock and the outer blocks compared to the weak incompatibility between the PS and PMMA end blocks. The reduction in interfacial free energy is the driving force which stabilizes these morphologies. Such a dominance of the relative incompatibilites of the components in controlling the overall morphology of triblock copolymers has not been reported so far.

Introduction

While a great deal of experimental as well as theoretical work deals with the ordered mesoscopic morphologies realized in microphase-separated AB and ABA block copolymers as well as $(AB)_n$ star block copolymers,[1,2] only a limited amount of information is available for ABC triblock copolymers. The study of ordered spherical, cylindrical, and lamellar morphologies in block copolymers dates back to the seventies and early eighties; the bicontinuous double-diamond morphology was only recognized in 1986.[3] For ABC triblock copolymers and blends with homopolymers, Riess et al.[4,5] gave a general scheme of possible types of morphologies. The proposed morphologies were composed of the structural features known from AB type block copolymers, i.e., spheres, cylinders, and lamellae. The volume fraction of the components was the main parameter determining the morphology. Some of these morphologies can be found in the literature. However, the experimental data for pure ABC triblock copolymers so far mainly show core-shell type structures, for example, sperical microdomains surrounded by a shell of the midblock,[5,6] as well as lamellar type morphologies in the case of more symmetric ABC block copolymers.[6-8] Recently, a highly ordered tricontinuous double-diamond morphology was reported from a P(I-*b*-S-*b*-VP) triblock copolymer.[9]

In the present paper we present morphological studies on block copolymers exhibiting new types of mesoscopic assemblies of higher structural order. The materials we are using are triblock copolymers of poly(styrene-*b*-ethylene-*co*-butylene-*b*-methyl methacrylate) (P(S-*b*-EB-*b*-MMA)) of molecular weights around 200 000, where we vary the fraction of the center block from 38 to 6 wt %, keeping the outer blocks approximately constant; i.e., the PS and the PMMA blocks are present in similar fractions. In the absence of the EB midblock (which is a fully hydrogenated 1,2-PB block), lamellar morphologies would be expected. Here we give a preliminary description of these new micromorphologies and a qualitative interpretation based on interfacial tensions. In the case of P(S-*b*-EB-*b*-MMA) the strong incompatibility between the EB midblock and the end blocks decisively determines the morphology and leads to unexpected highly ordered mesomorphic structures. A more detailed quantitative analysis with a calculation of the interfacial energies will be given in a forthcoming paper.[10]

Experimental Section

Anionic Synthesis of P(S-*b*-B-*b*-MMA). P(S-*b*-B-*b*-MMA) triblock copolymers were synthesized by sequential anionic polymerization in THF at low temperatures in the presence of lithium alkoxides. By this procedure, side reactions, especially during the polymerization of butadiene, are suppressed, and well-defined triblock copolymers without significant contamination of precursor polymers can be prepared. After polymerization of the styrene block at -80 °C, butadiene was polymerized at -10 °C. Before addition of MMA at -60 °C, the polybutadiene block is capped with 1,1-diphenylethylene to reduce the nucleophilicity of the living ends. After the polymerization of styrene and butadiene, aliquots were taken to recover PS precursor and P(S-*b*-B) intermediate for analytical purposes. A more detailed description of the synthesis including purification procedures is given elsewhere.[11] Table I shows the results of the analysis of three triblock copolymers.

P(S-*b*-EB-*b*-MMA). The quantitative hydrogenation of the 1,2-PB midblock was performed with tosyl hydrazide (4-fold molar excess relative to double bonds) in refluxing toluene.[10] The narrow molecular weight distribution is retained in the hydrogenated P(S-*b*-EB-*b*-MMA) triblock copolymers. Due to the enhanced thermal stability, the block copolymers can be annealed at high temperatures without cross-linking of the elastomeric center block.

Analytical Techniques. Analysis of the block copolymers was performed with GPC (THF, RI and UV detection, PS calibration), membrane osmometry, and ^{1}H-NMR. The molecular weight of the PS precursor can be accurately determined by GPC and membrane osmometry. The chemical composition of the triblock copolymers was determined by ^{1}H-NMR. Thus the most reliable M_n values for the P(S-*b*-B) intermediate and the triblock copolymer can be determined from the molecular weight of the PS precursor and the weight fractions of the blocks. Within experimental error, these calculated values were in agreement with the results from membrane osmometry.

Sample Preparation. Transparent bluish films of the pure triblock copolymers were slowly cast from $CHCl_3$ solution. For further equilibration, the dry films were annealed at 160 °C in vacuum for 5 days. Ultrathin sections were cut with an ultramicrotome equipped with a diamond knife. The rigidity of all samples was high enough to prepare high-quality ultrathin sections at room temperature. The ultrathin sections were mounted on gold grids and stained with RuO_4 vapor for TEM analysis.

Results

Figure 1 shows an electron micrograph of SEBM38 containing 38 wt % of ethylenebutylene rubber. As one

---

[*] To whom all correspondence should be addressed.

[†] Present address: Röhm GmbH, Darmstadt, Germany.

0024-9297/93/2226-2171$04.00/0

Table I
Characteristics of Triblock Copolymers[a]

		PS		P(S-*b*-B)		P(S-*b*-B-*b*-MMA)				
copolymer		$10^{-3}M_n$	M_w/M_n	$10^{-3}M_n$	M_w/M_n	$10^{-3}M_n$	M_w/M_n	w_{PS}	w_{PB}	w_{PMMA}
SEBM6	GPC	80	1.04	(93)	1.06	(165)	1.11	0.45	0.06	0.49
	osmom	88		96		225				
SEBM17	GPC	100	1.05	(148)	1.06	(205)	1.10	0.48	0.17	0.35
	osmom	108		145		238				
SEBM38	GPC	57	1.04	(135)	1.07	(189)	1.08	0.24	0.38	0.38
	osmom	64		175		245				

[a] The code of the SBM block copolymers denotes the weight fraction of the elastomeric midblock; parentheses indicate that GPC molecular weights of the P(S-*b*-B) intermediate and the triblock copolymer are somewhat too low due to PS calibration; w_{PS}, w_{PB}, and w_{PMMA} are the weight fractions of the components determined from ^{1}H-NMR.

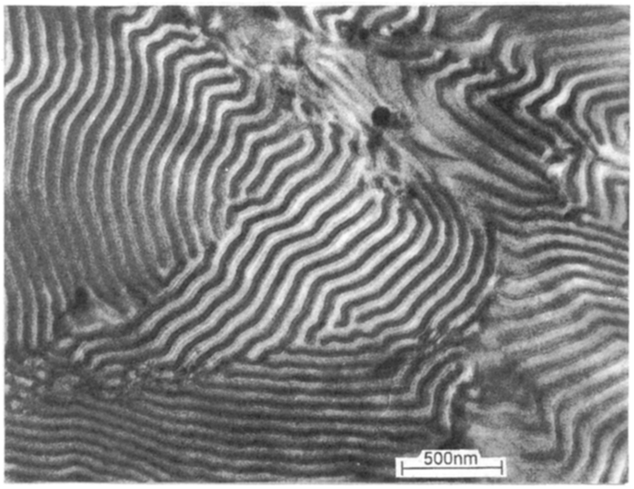

Figure 1. ABC lamellar morphology of the P(S-*b*-EB-*b*-MMA) triblock copolymer SEBM38: dark, PS lamellae; bright, PMMA lamellae; light gray, EB lamellae. Due to the weak contrast the EB and PMMA lamellae are not distinguishable at all positions.

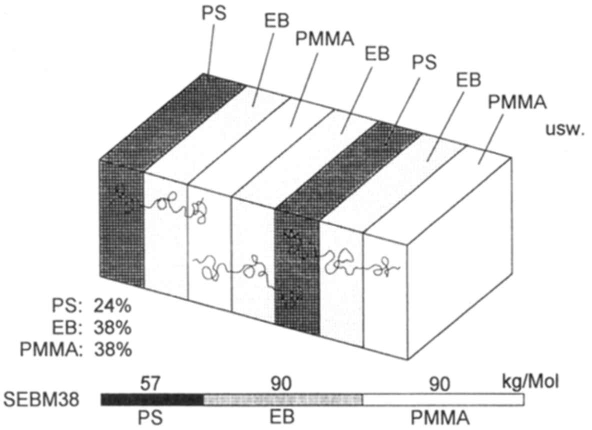

Figure 2. Schematic representation of the ABC lamellar morphology of the triblock copolymer SEBM38.

might expect, a lamellar morphology results in this case where the components are present in about equal amounts. Three different lamellae, as shown schematically in Figure 2, can be recognized on the electron micrograph. The PS lamellae appear dark because PS is readily attacked by RuO_4. PMMA does not react with RuO_4 under the applied staining conditions and therefore appears bright.[12] The intermediate EB lamellae are weakly stained and appear light gray. The overall morphology is a pure ABC lamellar structure.

The repeat unit of such an ABC lamellar structure perpendicular to the lamellae is ABCB. From the micrographs of SEBM38 the corresponding overall long period of PS–EB–PMMA–EB was determined to be ≈90–95 nm. From the volume fractions of the components (≈weight fractions), the thickness of the individual lamellae can be calculated to be $L_{PS} \approx 23$ nm, $L_{EB} = 2 \times \approx 18$ nm, and $L_{PMMA} \approx 35$ nm. For block copolymers in the strong segregation limit the dimensions L of the microdomains scale as[13]

$$L \sim M^{0.66} \tag{1}$$

To a first approximation we assume that the dimensions of the microdomains of P(S-*b*-EB-*b*-MMA) show this molecular weight dependence. In a symmetric P(S-*b*-MMA) diblock copolymer with a block molecular weight of 100k, the thickness of the PS and PMMA lamellae is 33 nm.[14] Taking this value, the thickness of the PS and PMMA lamellae in the triblock copolymer SEBM38 can be estimated with eq 1. For the 57k PS block $L_{PS}{}^{th} \approx 23$ nm is estimated, and for the 90k PMMA block $L_{PMMA}{}^{th} \approx 31$ nm is estimated. Within experimental error, these theoretical estimates compare well with the dimensions determined from the micrographs.

Reducing the length of the center block and keeping the overall PS/PMMA ratio constant (≈1:1) should retain the same all-lamellar morphology. In this case only the thickness of the EB lamella between the PS and PMMA lamellae would be reduced.

Figure 3a gives a micrograph of the triblock copolymer SEBM17 at moderate magnification. It can be seen that the gross morphology of SEBM17 is still lamellar. However, the lamellar surfaces are not flat anymore but have a very regular modulation. Figure 3b shows a micrograph at higher magnification. The surface modulation is the result of the formation of cylinders of the EB block at the PMMA/PS phase boundary. Figure 4 gives a schematic representation of this structure with a regular array of cylinders at the phase boundary between two lamellae.

Due to the staining conditions, the cylinder cross sections are clearly visible. No contrast developed between the EB microdomains and the PMMA lamellae, but the EB/PMMA phase boundary is stained to a larger extent.

The EB cylinders are located very regularly along the PS/PMMA lamellar interphase. The following parameters can be estimated from the analysis of these pictures: lamellar long period $L \approx 65$–70 nm, cylinder long period along the lamellar surface $L_c \approx 25$–30 nm, thickness of PS lamellae $L_{PS} \approx 35$–40 nm, thickness of PMMA lamella $L_{PMMA} \approx 30$–35 nm. From the average values of these data and the known composition (see Table I), the diameter of the EB cylinders is calculated to be 14 nm. This value is in good agreement with the diameters directly estimated from the electron micrographs $\phi_{EB} \approx 10$–15 nm.

Electron micrographs of SEBM6, which only contains about 6 wt % of EB of molecular weight 10k between two long PS (M_n = 80k) and PMMA (M_n = 90k) blocks, are shown in Figure 5 at two different magnifications. Though a gross lamellar morphology has to be expected based on the PS/PMMA composition, the micrographs show unambiguously a cylindrical morphology with PS cylinders (dark) in a PMMA matrix (light). Due to the low

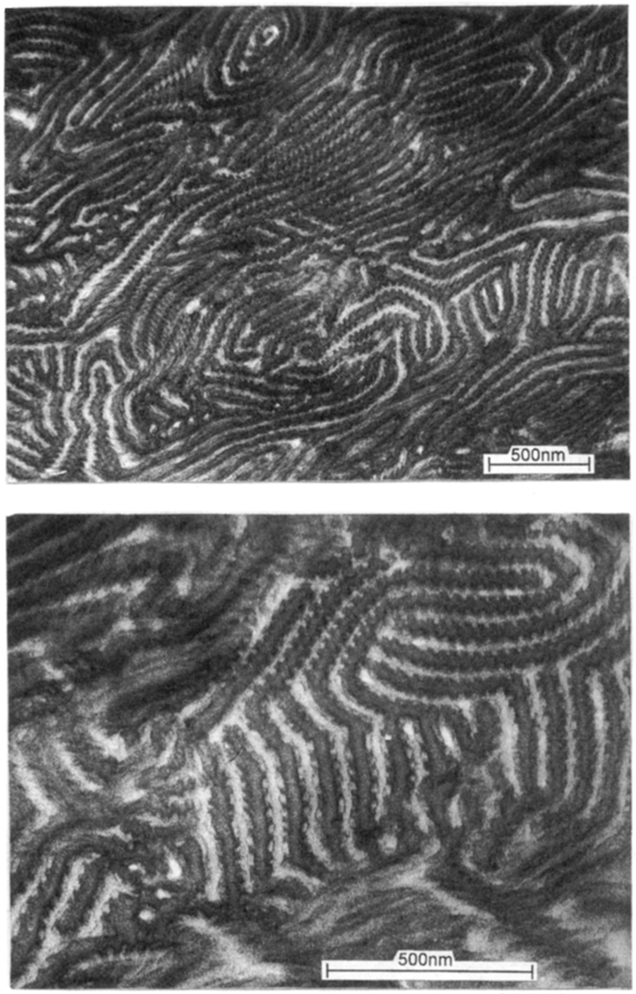

Figure 3. Morphology of the triblock copolymer SEBM17 at (a, top) moderate magnification and (b, bottom) higher magnification: dark, PS lamellae; bright, PMMA lamellae. The cross sections of the EB cylinders appear as spherical microdomains between the PS and PMMA lamellae.

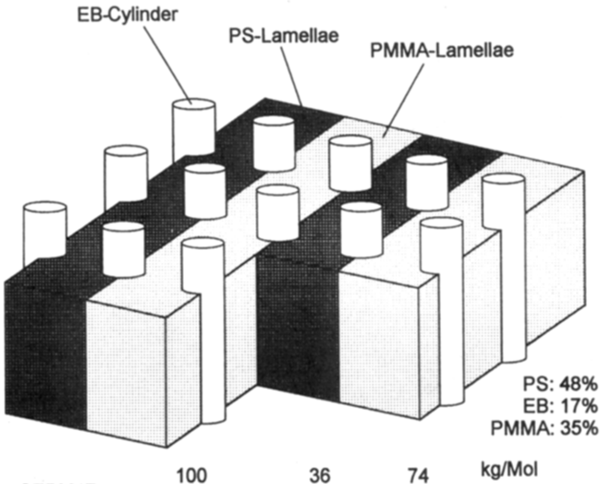

Figure 4. Schematic representation of the morphology of the triblock copolymer SEBM17 with EB cylinders between the PS and PMMA lamellae.

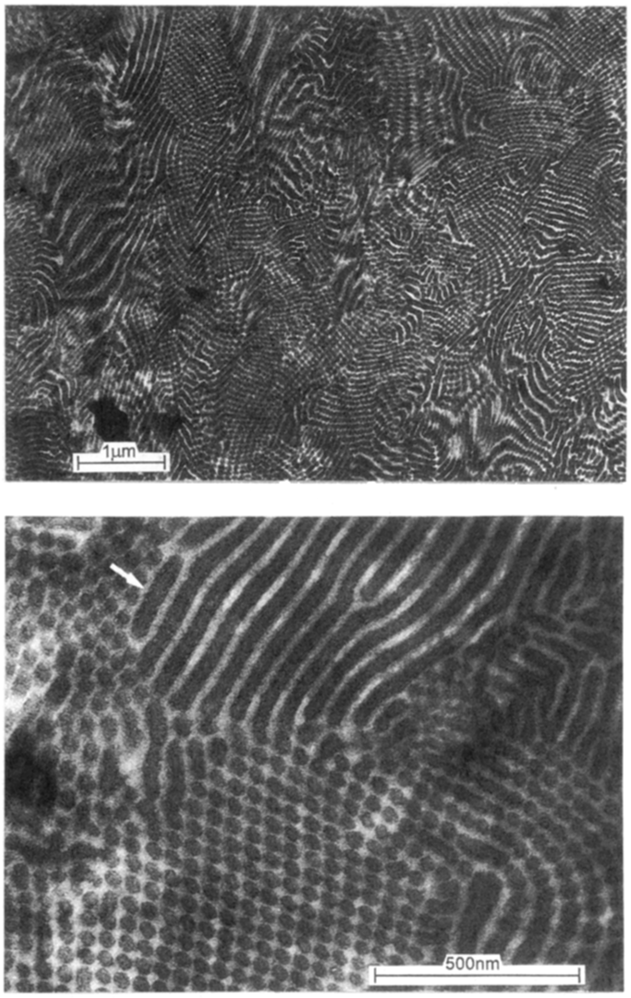

Figure 5. Morphology of the triblock copolymer SEBM6 at (a, top) moderate magnification and (b, bottom) higher magnification: dark, PS cylinders; bright, PMMA matrix. The EB rings around the PS cylinders can be recognized as small spherical cross sections on the surface of the PS domains (see arrow).

concentration of the elastomeric center blocks, the EB microdomains cannot be detected at the lower magnification (Figure 5a). However, Figure 5b shows very small regularly arranged circular structures in the sections along the cylinders. These regularly ordered EB microdomains along the PS cylinders are unambiguously recognized only at a few positions of the micrographs (see, for example, arrow in Figure 5b) because their diameter is only in the range between 5 and 10 nm (compared to an average thickness of the ultrathin sections of ≈50 nm). On the basis of the extremely regular arrangement and the constant diameter, which would not be expected if these circular structures result from spherical microdomains, we have to conclude that the EB midblock forms small isolated rings around the PS cylinders in the PMMA matrix. A schematic representation of this morphology is given in Figure 6.

Discussion

It is beyond the scope of the present paper to develop a quantitative explanation of the observed new morphologies; however, the fundamental idea appears to be very simple. In the most successful theories of block copolymers in the strong segregation limit of Helfand,[13] the contribution of the interface free energy is balanced by the requirement of retaining homogeneous segment density. The additional contribution resulting from the localization of the junctions between blocks at the interphase will be neglected in the present discussion.

The long spacing is mainly determined by the overall molecular weight, while different compositions mainly differ in the interface free energies calculated for the different morphologies. In the case of SEBM triblock copolymers the same arguments hold. However, in contrast to AB or ABA block copolymers, where only one binary interaction parameter determines the interface free

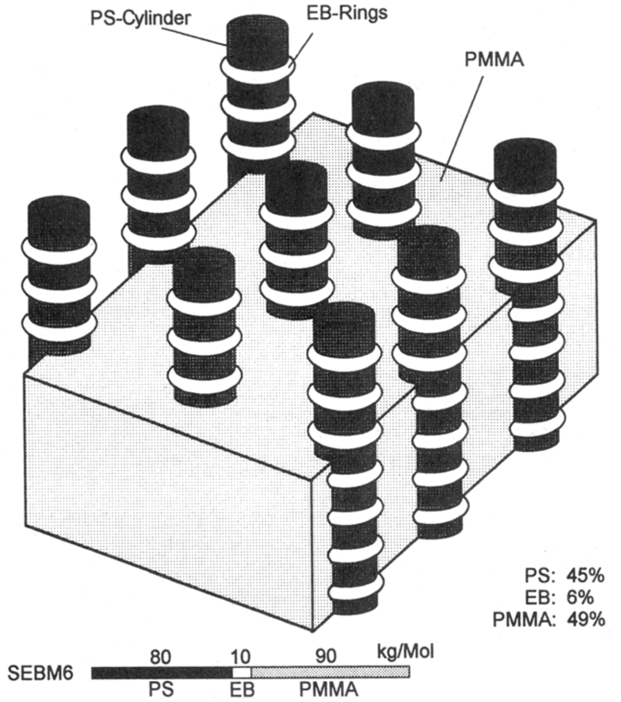

Figure 6. Schematic representation of the morphology of the triblock copolymer SEBM6 with PS cylinders dispersed in a PMMA matrix and isolated small EB rings around the PS cylinders.

Table II
Interfacial Tensions between the Components in P(S-*b*-EB-*b*-MMA)[15]

	components		
	PS/PMMA	PS/EB[a]	EB/PMMA[a]
γ(150 °C)/(dyn cm^{-1})	1.5	5.0	9.5

[a] Due to the lack of corresponding data for blends with EB, data for blends with polyethylene were taken from the literature as an approximation.

energy, three interaction parameters must be taken into account in ABC triblock copolymers. According to Helfand,[13] the interfacial tension γ in the strong segregation limit is related to the χ parameter according to

$$\gamma_{xy} \sim (\chi_{xy})^{1/2} \tag{2}$$

where xy are now the three combinations S/EB, EB/MMA, and S/MMA. Strong incompatibility (large positive χ) leads to high interfacial tensions.

Table II gives literature data for the interfacial tensions between the components of the triblock copolymers. The interfacial tension between EB/PMMA and EB/PS is much larger than between the "less" immiscible PS/PMMA pair. Thus the system will tend to minimize its overall interface free energy, which obviously most successfully can be achieved by reducing the surface of the EB domains. Calculation of the interface free energy of SEBM17 shows that cylinders located at the lamellar boundaries have a lower overall interface free energy than a corresponding ABC lamellar morphology.[10]

In principle, this situation has strong similarities to the behavior of homopolymer/copolymer blends (the so-called "copolymer effect" or "copolymer repulsion" model[16-18]), where miscibility results from strongly unfavorable interactions between segments within random copolymers. These unfavorable intramolecular repulsive interactions are replaced by less unfavorable interactions between segments of the copolymer and the homopolymer. In the case of P(S-*b*-EB-*b*-MMA), the highly ordered new morphologies are stabilized by the replacement of very unfavorable EB/PMMA and EB/PS interfacial contacts by less unfavorable PS/PMMA interfacial contacts.

Previous studies on the morphology of ABC triblock copolymers mainly considered systems like P(S-*b*-B-*b*-VP)[6,19] or P(I-*b*-S-*b*-VP)[8] (I = isoprene, VP = vinylpyridine) where the interaction between the outer blocks is more unfavorable than, or comparable to, the interactions between the outer blocks and the center block. In these systems, as in the case of triblock copolymers like P(S-*b*-I-*b*-MMA),[5] where the incompatibilities between the components are more balanced, mainly core–shell type and lamellar morphologies have been observed. Thus the morphologies controlled by the interface free energies between the three different components have been dismissed.

It is our feeling that the idea of controlling morphology by differences in the degree of incompatibility between the components may lead to the conception of other types of higher order block copolymer morphologies which are not yet imaginable. So far, we have not attempted to align the structures of SEBM17 into a mesoscopic monodomain as has been demonstrated for P(S-*b*-MMA) by Russell et al.[20] However, this possibility to generate higher order assemblies based on block copolymers appears to be very attractive.

Acknowledgment. This work has been supported by the BMFT and BASF through joint project no. 03M 40414 and by the German Science Foundation through Sonderforschungsbereich SFB 262—Glaszustand und Glasübergang nichtmetallischer amorpher Materialien. The authors are indebted to Mr. R. Würfel and Dr. I. Voigt-Martin (Institut für Physikalische Chemie, Mainz) for their advice and help at the electron microscope.

References and Notes

(1) Molau, G. E. In *Colloidal and Morphological Behavior of Block Copolymers*; Molau, G. E., Ed.; Plenum Press: New York, 1971.
(2) Quirk, R. P.; Kinning, D. J.; Fetters, L. J. *Comp. Polym. Sci.* **1989**, *7*, 1.
(3) Kinning, D. J.; Thomas, E. L.; Alward, D. B.; Fetters, L. J.; Handlin, D. L. *Macromolecules* **1986**, *19*, 1288, 2197.
(4) Riess, G. In *Thermoplastic Elastomers. A Comprehensive Review*; Ledge, N. R., Holden, G., Schroeder, H. E., Eds.; Hanser: Munich, 1987; Chapter 12.2, p 325.
(5) Riess, G.; Schlienger, M.; Marti, S. *J. Macromol. Sci., Phys.* **1989**, *B17* (2), 355.
(6) Arai, K.; Kotaka, T.; Kitano, Y.; Yoshimura, K. *Macromolecules* **1980**, *13*, 1670.
(7) Matsushita, Y.; Choshi, H.; Fujimoto, T.; Nagasawa, M. *Macromolecules* **1980**, *13*, 1053.
(8) Mogi, Y.; Kotsuji, H.; Kaneko, Y.; Mori, K.; Matsushita, Y.; Noda, I. *Macromolecules* **1992**, *25*, 5408.
(9) Mogi, Y.; Mogi, K.; Matsushita, Y.; Noda, I. *Macromolecules* **1992**, *25*, 5412.
(10) Auschra, C.; Stadler, R. *Macromolecules*, in preparation.
(11) Auschra, C.; Stadler, R. *Polym. Bull.*, in press.
(12) Trent, J. S.; Scheinbeim, J. I.; Couchman, P. R. *Macromolecules* **1983**, *16*, 589.
(13) Helfand, E.; Wasserman, Z. R. *Macromolecules* **1975**, *8*, 552; **1976**, *9*, 879; **1978**, *11*, 960; **1980**, *13*, 994.
(14) Green, P. F.; Russell, T. P.; Jerome, R.; Granville, M. *Macromolecules* **1988**, *21*, 3266.
(15) *Polymer Handbook*, 3rd ed.; Brandrup, J., Immergut, E. H., Eds.; J. Wiley & Sons: New York, 1989.
(16) Kambour, R. P.; Bendler, J. T.; Bopp, R. C. *Macromolecules* **1983**, *16*, 753.
(17) Silvestre, C.; Martuscelli, E.; Karasz, F. E.; MacKnight, W. J. *Polymer* **1987**, *28*, 1190.
(18) ten Brinke, G.; Karasz, F. E.; MacKnight, W. J. *Macromolecules* **1983**, *16*, 1827.
(19) Kudose, I.; Kotaka, T. *Macromolecules* **1984**, *17*, 2325.
(20) Russell, T. P.; Mayers, A. M. *Polym. Prepr. (Am. Chem. Soc., Div. Polym. Chem.)* **1992**, *33* (2), 618.